



Universiteit  
Leiden  
The Netherlands

## Technical developments for clinical MR applications at 7 T

Versluis, M.J.

### Citation

Versluis, M. J. (2013, March 6). *Technical developments for clinical MR applications at 7 T*. Retrieved from <https://hdl.handle.net/1887/20590>

Version: Corrected Publisher's Version

License: [Licence agreement concerning inclusion of doctoral thesis in the Institutional Repository of the University of Leiden](#)

Downloaded from: <https://hdl.handle.net/1887/20590>

**Note:** To cite this publication please use the final published version (if applicable).

Cover Page



Universiteit Leiden



The handle <http://hdl.handle.net/1887/20590> holds various files of this Leiden University dissertation.

**Author:** Versluis, Maarten Jan

**Title:** Technical developments for clinical MR applications at 7 T

**Issue Date:** 2013-03-06

# 3

## **Right Coronary MR Angiography at 7 Tesla: A Direct Quantitative and Qualitative Comparison with 3 Tesla in Young Healthy Volunteers**

*S.G.C. van Elderen  
M.J. Versluis  
J.J.M. Westenberg  
H. Agarwal  
N.B. Smith  
M. Stuber  
A. de Roos  
A.G. Webb*

**ABSTRACT***Purpose:*

To objectively compare quantitative parameters related to image quality attained at coronary magnetic resonance (MR) angiography of the right coronary artery (RCA) performed at 7 Tesla (T) and 3 T.

*Materials and Methods:*

Institutional review board approval was obtained, and volunteers provided signed informed consent. Ten healthy adult volunteers (mean age  $\pm$  standard deviation, 25 years  $\pm$  4; seven men, three women) underwent navigator-gated three-dimensional MR angiography of the RCA at 7 T and 3 T. For 7 T, a custom-built quadrature radiofrequency transmit-receive surface coil was used. At 3 T, a commercial body radiofrequency transmit coil and a cardiac coil array for signal reception were used. Segmented k-space gradient-echo imaging with spectrally selective adiabatic fat suppression was performed, and imaging parameters were similar at both field strengths. Contrast-to-noise ratio between blood and epicardial fat; signal-to-noise ratio of the blood pool; RCA vessel sharpness, diameter, and length; and navigator efficiency were quantified at both field strengths and compared by using a Mann-Whitney U test.

*Results:*

The contrast-to-noise ratio between blood and epicardial fat was significantly improved at 7 T when compared with that at 3 T ( $87 \pm 34$  versus  $52 \pm 13$ ;  $P = .01$ ). Signal-to-noise ratio of the blood pool was increased at 7 T ( $109 \pm 47$  versus  $67 \pm 19$ ;  $P = .02$ ). Vessel sharpness obtained at 7 T was also higher ( $58\% \pm 9$  versus  $50\% \pm 5$ ;  $P = .04$ ). At the same time, RCA vessel diameter and length and navigator efficiency showed no significant field strength dependent difference.

*Conclusion:*

In our quantitative and qualitative study comparing in vivo human imaging of the RCA at 7 T and 3 T in young healthy volunteers, parameters related to image quality attained at 7 T equal or surpass those from 3 T.

## INTRODUCTION

Currently, relatively few (approximately 40) 7 T magnetic resonance (MR) imaging systems are available for human use, and most of them are situated in research centers. High-field-strength cardiac MR imaging initially was thought to be problematic due to magnetic field inhomogeneity and specific absorption rate constraints. Furthermore, contemporary commercial 7 T units are not routinely equipped with body radiofrequency (RF) transmit coils or surface RF receive coils. Despite these major challenges, a number of research groups already have demonstrated the feasibility of cardiac imaging at 7 T and beyond (1–5). Initial attempts focusing on coronary artery imaging at 7 T showed that these barriers can be removed successfully, and initial *in vivo* human images were promising (6). Although these early 7 T studies were conducted by using single-channel RF transmit-receive coil architecture, recent advances in surface coil technology seem particularly promising. However, although an improvement in image quality may be expected at higher magnetic field strength (7), there have been no reports, to our knowledge, on cardiac MR imaging studies in which investigators directly and objectively compare parameters related to image quality at 7 T with those obtained at lower field strength. Therefore, the purpose of our study was to objectively compare quantitative parameters related to image quality attained at coronary MR angiography of the right coronary artery (RCA) performed at 7 T and 3 T.

## MATERIALS AND METHODS

Our study was approved by our institutional review board, and all volunteers provided signed informed consent. Three-dimensional (3D) MR angiography of the right coronary system was performed in 10 healthy young adult volunteers (mean age  $\pm$  standard deviation, 25 years  $\pm$  4; seven men, three women) who underwent imaging at 7 T and 3 T (Achieva; Philips Healthcare, Best, the Netherlands) in a prospective study design. For practical reasons, 7 T imaging always occurred before 3 T imaging. Coronary MR Angiography was performed with prospective navigator technology and vector electrocardiographic (ECG) triggering (8). All volunteers underwent imaging in a head-first, supine position. None of the volunteers received nitroglycerin before MR imaging. The mean interval between the two examinations was 8 weeks  $\pm$  5.

### *Imaging at 7 T*

A quadrature transmit-receive surface coil consisting of two overlapping

loops (13-cm diameter each) was constructed in-house (Fig 1). The coil size is larger than described previously (4, 6) to improve volumetric coverage. First, non-ECG-triggered scout images in coronal, transverse, and sagittal orientations were acquired to plan subsequent images and to localize the two-dimensional selective navigator. At 7 T, the navigator was placed at the lung-heart interface because of the limited sensitive volume of the surface coil. Second, ECG-triggered, breath-hold multisection transverse cine scout imaging was performed for both the determination of the period of minimal coronary motion (trigger delay) and the volume targeting of the 3D stack in parallel with the middiastolic RCA. Finally, volume-targeted coronary MR angiography was performed by using a 3D segmented k-space gradient-echo imaging technique (parameters are in Table 1) combined with a spectrally selective adiabatic inversion-recovery pulse (inversion time, 200 msec) for fat saturation. First-order local volume shimming at the anatomic level of the RCA was performed in all cases.



**Figure 1:RF coil**

Custom-built quadrature RF transmit-receive surface coil consisting of two 13-cm elements used for our study at 7 T.

### *Imaging at 3 T*

On the 3 T system, the body coil was used for RF transmission, with a commercial six-element cardiac coil array for signal reception. Scout imaging included free-breathing, retrospectively ECG-gated, two-dimensional cine balanced fast gradient-echo imaging in a horizontal long-axis view (four-chamber) to determine the trigger delay. Furthermore, ECG-triggered free-breathing navigator-gated and corrected 3D gradient-echo whole-heart imaging was performed for the anatomic localization of the RCA. After scout imaging, two coronary imaging sequences were performed at 3 T with different naviga-

tor localization in random order: (a) with navigator localization at the lung-heart interface (navigator at heart) and (b) with navigator localization at the lung-liver interface (navigator at liver). Both 3 T coronary imaging sequences consisted of a 3D segmented k-space gradient-echo technique with spectrally selective adiabatic inversion recovery (inversion time, 150 msec) for fat saturation. The coronary MR angiography imaging parameters were similar (Table 1) at both field strengths to support a fair quantitative comparison.

Field strength	7 Tesla	3 Tesla	3 Tesla
Sequence	3D gradient echo	3D gradient echo	3D gradient echo
Navigator position/correction factor	Lung-Heart interface / 1.0	Lung-Heart interface / 1.0	Lung-Liver interface / 0.6
Coil	Quadrature two-element surface coil transmit/receive	Body coil transmit / six-element phased array receive	Body coil transmit / six-element phased array receive
Fat suppression	Adiabatic SPIR	Adiabatic SPIR	Adiabatic SPIR
TR (ms)	4.3	4.3	4.3
TE (ms)	1.38	1.38	1.38
TI (ms)	200	150	150
Acquired voxel size (mm <sup>3</sup> )	0.82x0.86x2.00	0.82x0.86x2.00	0.82x0.86x2.00
Reconstructed voxel size (mm <sup>3</sup> )	0.82x0.82x1.00	0.82x0.82x1.00	0.82x0.82x1.00
Number of slices	30	30	30
Field of view (mm <sup>2</sup> )	420x268	420x269	420x269
Matrix	512x312	512x312	512x312
Flip angle (°)	15	15	15
Acquisition window (ms)	107	108	108

*Data Analysis*

Images were processed and analyzed by using the Soap-Bubble tool (9). Both a visual qualitative description and a direct quantitative comparison between 7 T and 3 T images were performed. All data analyses were performed by one physician (S.G.C.v.E., with 4 years of experience in cardiac MR

imaging) with the supervision of a senior researcher (M.S., with 18 years of experience in cardiac MR imaging).

The following parameters were measured: contrast-to-noise ratio (CNR) between the blood pool and the epicardial fat, signal-to-noise ratio (SNR) of the blood pool, RCA vessel sharpness and diameter of the first 4 cm, and visible vessel length. The CNR was defined as the difference in signal intensity between a manually placed region of interest (ROI) in the aortic root (mean ROI area,  $1.80 \text{ cm}^2 \pm 0.60$ ) near the offshoot of the RCA, and that of an ROI placed in the epicardial fat adjacent to the proximal RCA (mean ROI area,  $0.90 \text{ cm}^2 \pm 0.61$ ), divided by the standard deviation of the background signal from an ROI positioned anterior to the chest wall (noise; mean ROI area,  $9.95 \text{ cm}^2 \pm 3.98$ ). The SNR was calculated for the blood signal intensity in the described ROI localized in the aortic root. The average signal intensity from this ROI was divided by the noise. Vessel sharpness was measured by using signal intensity gradients perpendicular to the 3D course of the RCA and was calculated for the proximal 4 cm of the RCA (9). The RCA vessel length was measured manually, and both vessel sharpness and diameter for the proximal 4 cm of the RCA were calculated automatically by the software.

### *Statistical Analysis*

Data are presented as mean  $\pm$  standard deviation. Comparisons were made between the results obtained at 7 T and 3 T and between the results obtained with the different navigator positions at 3 T. For comparisons, a non-parametric Mann-Whitney U test was used.  $P < .05$  was considered to indicate a statistically significant difference.

## **RESULTS**

Coronary MR angiography was performed successfully in all volunteers at both field strengths. At 7 T, one study volunteer complained about vertigo while the table was moving. All quantitative findings are listed in Table 2. Total time in the magnet was on average 30 minutes at 7 T and 20 minutes at 3 T.

Figures 2–4 illustrate example coronary MR angiography reformations obtained at 7 T and at 3 T. All images show high signal intensity of the coronary artery lumen, while that of the surrounding epicardial fat is suppressed. At 7 T, suppression of the epicardial fat appears visually improved when compared with that at 3 T (Fig 2). Consistent with these findings, quantitative CNR between the blood pool and epicardial fat was significantly improved at 7 T



(7 T versus 3 T navigator at heart, P = .013; 7 T versus 3 T navigator at liver, P = .009).

**Table 2: Quantitative results obtained from 10 healthy volunteers**

	7 Tesla, navigator on lung-heart	3 Tesla, navigator on lung-heart	3 Tesla, navigator on lung-liver
<b>CNR</b>	87.5 ± 33.9*	51.7 ± 12.7	47.8 ± 15.2
<b>SNR blood pool</b>	109.2 ± 46.9*	66.9 ± 19.4	67.2 ± 24.9
<b>RCA vessel sharpness (%)</b>	58.3 ± 8.9*	49.7 ± 5.1	48.9 ± 7.5
<b>RCA vessel length (cm)</b>	7.24 ± 2.34	8.21 ± 2.19	7.99 ± 2.73
<b>RCA diameter, first 4 cm (mm)</b>	2.97 ± 0.27	3.07 ± 0.38	3.07 ± 0.37
<b>Navigator efficiency (%)</b>	54 ± 20	53 ± 20	46 ± 14
<b>Acquisition time (sec)</b>	469 ± 225	410 ± 180	470 ± 191
<b>Heart rate (beats / min)</b>	70 ± 15	67 ± 10	69 ± 10

\* significantly different from 3 T (p<0.05). CNR: contrast-to-noise ratio between proximal coronary blood pool and surrounding perivascular tissue; RCA: right coronary artery; SNR: signal-to-noise ratio

Visually, the contrast between the myocardium and the blood pool in the left ventricle is rather shallow at 7 T as shown in Figures 3 and 4.4. When compared with that at 3 T, the SNR of the blood pool measured on the 7 T images was 60% higher (7 T versus 3 T navigator at heart, P = .023; 7 T versus 3 T navigator at liver, P = .027). Improved delineation of the RCA at 7 T is visible in Figure 3, with good depiction of RCA branches and distal segments. Consistent with these findings, objective vessel sharpness analysis demonstrated improved quantitative vessel conspicuity at 7 T (versus 3 T navigator at heart, P = .038; versus 3 T navigator at liver; P = .031). Even though constraints related to the B1 field and coil sensitivity adversely affected the signal more distant to the surface transmit-receive coil at 7 T (Figs 2–4), there was no significant difference in vessel length (7 T versus 3 T navigator at heart, P = .233; 7 T versus 3 T navigator at liver, P = .414) or vessel diameter (7 T versus 3 T navigator at heart, P = .653; 7 T versus 3 T navigator at liver, P = .567) measurements among the images from the different field strengths. Navigator efficiency (7 T versus 3 T navigator at heart, P = .970; 7 T versus 3 T navigator at liver, P = .272) and total data acquisition time (7 T versus 3 T

navigator at heart,  $P = .520$ ; 7 T versus 3 T navigator at liver,  $P = .821$ ) also were not field strength dependent. No significant difference in CNR between the blood pool and epicardial fat, SNR of the blood pool, RCA vessel sharpness, vessel length, vessel diameter, navigator efficiency, or acquisition time was found between the 3 T images acquired with the different navigator localizations.

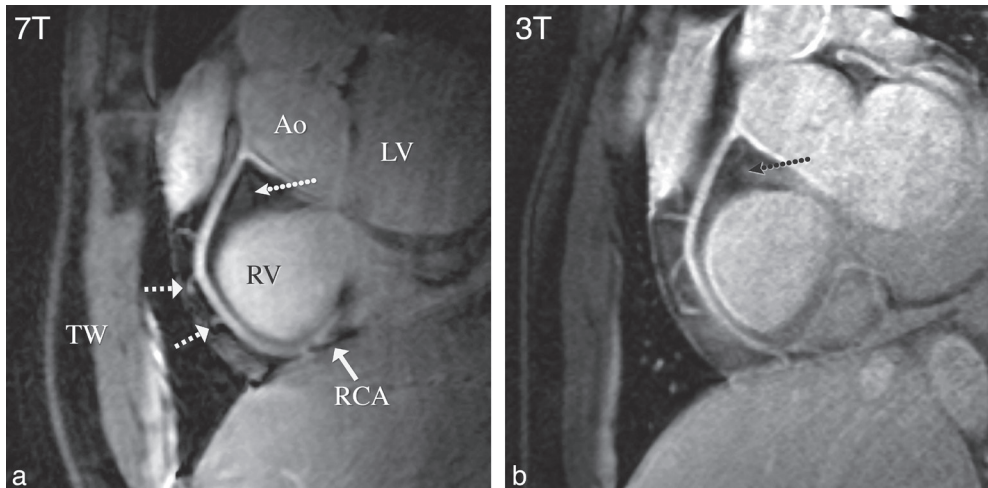


**Figure 2: Coronary MR angiograms of the RCA.**

Obtained at (a) 7 T and (b) 3 T in the same healthy 18-year-old man (double oblique volume targeted plane parallel to the RCA). Improved suppression of the epicardial fat (long dotted arrow) with high contrast between the blood and epicardial fat is visible at 7 T. At both field strengths, a number of small branching vessels are depicted (short dashed arrows). Also at 7 T, a long portion of the RCA is visible (solid arrow = distal part of RCA). Ao = aortic root, LV = left ventricle, RV = right ventricle, TW = thoracic wall.

## DISCUSSION

In our study comparing 7 T and 3 T RCA coronary MR angiography in young healthy volunteers, we found improved CNR between the blood pool and the epicardial fat, enhanced SNR of the blood pool, and increased vessel sharpness at 7 T. These findings may have implications, since vessel conspicuity and well-defined borders of the coronary arteries support improved identification of significant coronary artery stenoses.

The results of a multicenter study indicate that multidetector computed tomography (CT) is highly promising and superior to MR angiography for the noninvasive evaluation of significant proximal coronary stenoses (10). However, the most recent data from a coronary MR angiography multicenter trial (11) demonstrate substantial progress, and further improvement in SNR di-

agnostic quality approaching that of CT angiography may be expected soon; therefore, the development of new MR imaging methodology at higher magnetic field strength is of particular interest.

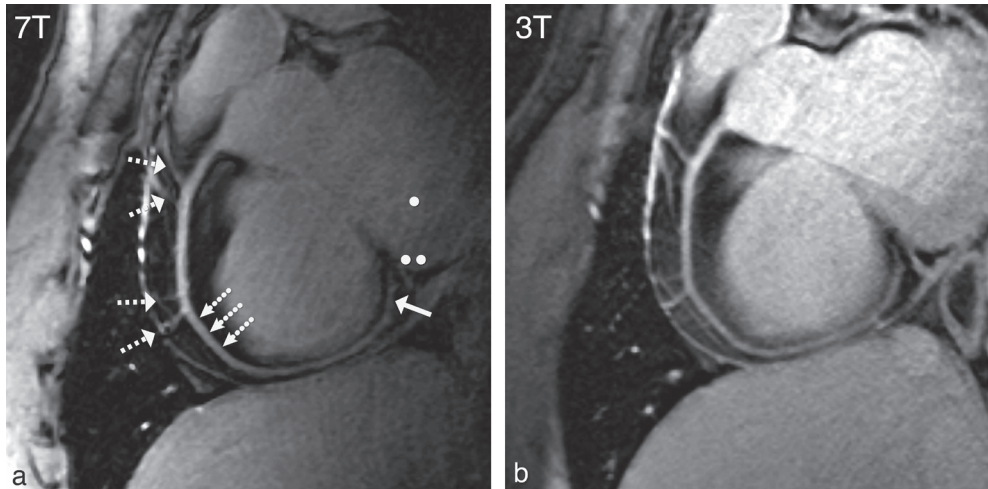


**Figure 3: Coronary MR angiograms of the RCA.**

Double oblique volume targeted plane parallel to the RCA in a healthy 26-year-old man display a high visual vessel definition (dotted arrows) in (a) the 7 T image compared with that at (b) 3 T. At 7 T, contrast is limited between the myocardium ( . ) and the blood pool ( .. ). Multiple RCA side branches (dashed arrows) and distal parts of the RCA (solid arrow) are depicted clearly at both field strengths.

Approximately a twofold increase in SNR is predicted at 7 T when compared with 3 T (7, 12), whereas a 60% SNR improvement was found in our study, which may be explained with the prolonged  $T_1$  at 7 T and the depth penetration of the RF transmit-receive coil, which was clearly inferior to that at 3 T. However, a significant 60% increase in SNR with a simple coil design is encouraging and emphasizes the need for further developments in coil technology. Recent advances in RF transmit arrays (2, 3) are a step in this direction. Findings from previous studies in which investigators compared 1.5 T and 3 T coronary MR angiography (13–15) clearly demonstrated that the expected 100% improvement in SNR could not be obtained. At 7 T, the lack of commercially available RF coils and the only recent availability of 7 T for whole-body human use constitute additional 7 T–specific limitations. Despite these limitations, the reported 60% improvement in SNR, when going from 3 T to 7 T, is consistent with that reported for direct 1.5 T versus 3 T.

Our findings of increased vessel sharpness at 7 T suggest that motion suppression works effectively at 7 T, since vessel sharpness depends on the performance of ECG triggering and the respiratory navigator. Two similar ima-

ging sequences with different navigator localizations were performed at 3 T to exclude the influence of navigator localization on the quantitative parameters related to image quality. Consistent with earlier findings (16), no navigator-dependent quantitative differences were observed.

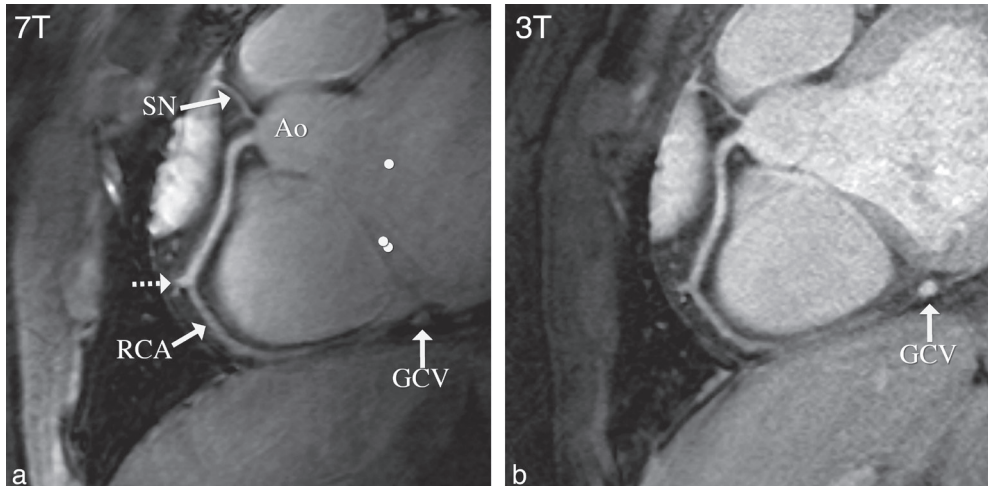


**Figure 4: Sinoatrial nodal artery (SN) and a proximal branch of the RCA.**

Image obtained in a double oblique volume targeted plane parallel to the RCA in a healthy 28-year-old man. (a) At 7 T, there is not much difference in signal intensity between the blood pool ( . ) and the myocardium ( .. ). (b) At 3 T, this contrast is slightly improved. On b , the great cardiac vein (GCV ) can be identified easily, but this structure is less visible on a , likely because of shortened T2\* at 7 T, as well as limited surface coil RF penetration. Ao = aortic root, dashed arrow = RCA side branch.

The results from the RCA vessel length and diameter measurements were similar for both field strengths. This finding suggests that coverage and RF penetration of the surface coil at 7 T may not be limiting factors for visualization of the RCA.

The situation for the left coronary system is different. On the one hand, the penetration depth of the current transmit-receive coil is limited, so parts of the left coronary system may not be visualized easily. On the other hand, an enhancement of the contrast between myocardium and the blood pool is mandatory for visualizing the left coronary system. At 3 T, such contrast enhancement has been obtained with adiabatic T<sub>2</sub> preparation (17) or with the combination of extracellular contrast agents and inversion recovery (18). However, at 7 T, specific absorption rate constraints preclude the use of the T<sub>2</sub> preparation, and alternative 7 T–specific solutions with or without contrast agents remain to be explored. Finally, although a 60% increase in SNR was obtained at 7 T, we have not used this gain for increased spatial resolu-

tion. However, the objective of our work was a direct, quantitative, objective comparison with 3 T.

In conclusion, although substantial challenges are associated with 7 T cardiac MR imaging, a number of them have been addressed successfully. In our study directly comparing in vivo human imaging of the RCA at 7 T and 3 T in young healthy volunteers, quantitative parameters related to image quality attained at 7 T equal or surpass those from 3 T. Our results clearly warrant further evaluation in patients with coronary artery disease to assess the potential of our 7 T approach for the visualization of luminal RCA disease. Future work will concentrate on refinements in coil technology and contrast generation to support concomitant imaging of the left coronary system.

### **ACKNOWLEDGMENTS**

Supported by the Dutch Organization for Scientific Research (Nederlandse Organisatie voor Wetenschappelijk Onderzoek [NWO]).

## REFERENCES

1. Maderwald S, Orzada S, Schäfer LC, Bitz AK, Brote I, Kraff O, Theysohn JM, Ladd ME, Ladd SC, Quick HH. 7T Human in vivo cardiac imaging with an 8-channel transmit/receive array. In: Proceedings of the 17th Annual Meeting of ISMRM. 2009.
2. Snyder CJ, DelaBarre L, Metzger GJ, Moortele P-F van de, Akgun C, Ugurbil K, Vaughan JT. Initial results of cardiac imaging at 7 tesla. *Magnetic Resonance in Medicine* 2009 ;61:517–524.
3. Vaughan JT, Snyder CJ, DelaBarre LJ, Bolan PJ, Tian J, Bolinger L, Adriany G, Andersen P, Strupp J, Ugurbil K. Whole-body imaging at 7T: Preliminary results. *Magnetic Resonance in Medicine* 2009 ;61:244–248.
4. Versluis MJ, Tsekos N, Smith NB, Webb AG. Simple RF design for human functional and morphological cardiac imaging at 7 tesla. *Journal of Magnetic Resonance* 2009 ;200:161–166.
5. Frauenrath T, Hezel F, Heinrichs U, Kozerke S, Utting JF, Kob M, Butenweg C, Boesiger P, Niendorf T. Feasibility of cardiac gating free of interference with electromagnetic fields at 1.5 Tesla, 3.0 Tesla and 7.0 Tesla using an MR-stethoscope. *Invest Radiol* 2009 ;44:539–547.
6. Elderen SGC van, Versluis MJ, Webb AG, Westenberg JJM, Doornbos J, Smith NB, Roos A de, Stuber M. Initial results on in vivo human coronary MR angiography at 7 T. *Magnetic Resonance in Medicine* 2009 ;62:1379–1384.
7. Wen H, Denison TJ, Singerman RW, Balaban RS. The intrinsic signal-to-noise ratio in human cardiac imaging at 1.5, 3, and 4 T. *J. Magn. Reson.* 1997 ;125:65–71.
8. Fischer SE, Wickline SA, Lorenz CH. Novel real-time R-wave detection algorithm based on the vectorcardiogram for accurate gated magnetic resonance acquisitions. *Magn Reson Med* 1999 ;42:361–370.
9. Etienne A, Botnar RM, Muiswinkel AMC van, Boesiger P, Manning WJ, Stuber M. Soap-Bubble visualization and quantitative analysis of 3D coronary magnetic resonance angiograms. *Magnetic Resonance in Medicine* 2002 ;48:658–666.
10. Miller JM, Rochitte CE, Dewey M, Arbab-Zadeh A, Niinuma H, Gottlieb I, Paul N, Clouse ME, Shapiro EP, Hoe J, Lardo AC, Bush DE, de Roos A, Cox C, Brinker J, Lima JAC. Diagnostic performance of coronary angiography by 64-row CT. *N. Engl. J. Med.* 2008 ;359:2324–2336.
11. Kato S, Kitagawa K, Ishida N, Ishida M, Nagata M, Ichikawa Y, Katahira K, Matsumoto Y, Seo K, Ochiai R, Kobayashi Y, Sakuma H. Assessment of coronary artery disease using magnetic resonance coronary angiography: a national multicenter trial. *J. Am. Coll. Cardiol.* 2010 ;56:983–991.
12. Vaughan JT, Garwood M, Collins CM, Liu W, DelaBarre L, Adriany G, Andersen P, Merkle H, Goebel R, Smith MB, Ugurbil K. 7T vs. 4T: RF power, homogeneity, and signal-to-noise comparison in head images. *Magn Reson Med* 2001 ;46:24–30.
13. Bi X, Deshpande V, Simonetti O, Laub G, Li D. Three-dimensional breathhold SSFP coronary MRA: a comparison between 1.5T and 3.0T. *J Magn Reson Imaging* 2005 ;22:206–212.
14. Sommer T, Hackenbroch M, Hofer U, Schmiedel A, Willinek WA, Flacke S, Gieseke J, Träber F, Fimmers R, Litt H, Schild H. Coronary MR angiography at 3.0 T versus that at 1.5 T: initial results in patients suspected of having coronary artery disease. *Radiology* 2005 ;234:718–725.

15. Yang PC, Nguyen P, Shimakawa A, Brittain J, Pauly J, Nishimura D, Hu B, McConnell M. Spiral magnetic resonance coronary angiography--direct comparison of 1.5 Tesla vs. 3 Tesla. *J Cardiovasc Magn Reson* 2004 ;6:877–884.
16. Stuber M, Botnar RM, Danias PG, Kissinger KV, Manning WJ. Submillimeter three-dimensional coronary MR angiography with real-time navigator correction: comparison of navigator locations. *Radiology* 1999 ;212:579–587.
17. Botnar RM, Stuber M, Danias PG, Kissinger KV, Manning WJ. Improved coronary artery definition with T2-weighted, free-breathing, three-dimensional coronary MRA. *Circulation* 1999 ;99:3139–3148.
18. Bi X, Li D. Coronary arteries at 3.0 T: Contrast-enhanced magnetization-prepared three-dimensional breathhold MR angiography. *J Magn Reson Imaging* 2005 ;21:133–139.

